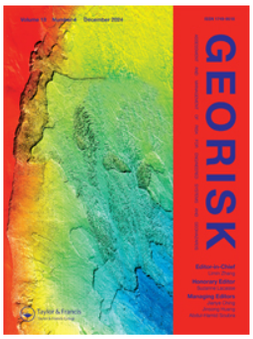

Georisk: Assessment and Management of Risk for Engineered Systems and Geohazards

ISSN: (Print) (Online) Journal homepage: www.tandfonline.com/journals/ngrk20

# Updating reliability of pile groups with load tests considering spatially variable soils

Yuting Zhang, Jinsong Huang, Jiawei Xie, Anna Giacomini & Cheng Zeng

**To cite this article:** Yuting Zhang, Jinsong Huang, Jiawei Xie, Anna Giacomini & Cheng Zeng (2024) Updating reliability of pile groups with load tests considering spatially variable soils, Georisk: Assessment and Management of Risk for Engineered Systems and Geohazards, 18:4, 750-764, DOI: 10.1080/17499518.2024.2328189

**To link to this article:** https://doi.org/10.1080/17499518.2024.2328189



Published online: 18 Mar 2024.

GEORISK
2024, VOL. 18, NO. 4, 750–764
https://doi.org/10.1080/17499518.2024.2328189

Taylor & Francis
Taylor & Francis Group



# Updating reliability of pile groups with load tests considering spatially variable soils

Yuting Zhang, Jinsong Huang, Jiawei Xie, Anna Giacomini and Cheng Zeng

Discipline of Civil, Surveying and Environmental Engineering, Priority Research Centre for Geotechnical Science and Engineering, The University of Newcastle, Callaghan, Australia

**ABSTRACT**

This paper proposes a rigorous framework to update the reliability of pile groups based on load tests. The proposed approach enables the consideration of the spatial variability of soils, which is disregarded in previous studies. To achieve this, the random finite difference method (RFDM) is utilised to assess the group efficiency, individual pile capacities, and the correlation between individual pile capacities in spatially variable soils. Subsequently, Bayes' theorem is employed to update individual pile capacities based on load test results, taking into account the correlation between individual pile capacities. Finally, the reliability of pile groups is evaluated based on the group efficiency and updated individual pile capacities. An axially loaded pile group in undrained clays is utilised for demonstration. Results indicate that neglecting the spatial variability of soils may lead to unrealistic assessments of the reliability of pile groups. Specifically, in cases where all piles fail, the ignorance of spatial variability results in an overconservative design. Conversely, in cases where one or more piles pass, it leads to an unconservative design.

**ARTICLE HISTORY**
Received 22 June 2023
Accepted 6 February 2024

**KEYWORDS**
Pile load tests; reliability; pile group; random finite difference method; Bayes' theorem

## 1. Introduction

Uncertainties exist in the design and construction of pile foundations. For example, the design parameters are commonly established by limited site investigations and tests that are associated with measurement errors (Länsivaara, Phoon, and Ching 2021). Besides, empirical methods, such as static analysis and dynamic formulas, are used to determine pile capacity during the design phase, subject to model uncertainties (Phoon and Tang 2019). Furthermore, construction methods and workmanship can vary significantly from pile to pile, further exacerbating uncertainties. To address these uncertainties and verify that the pile has sufficient capacity, pile load tests are commonly utilised. The adoption of load tests provides a more accurate estimation of pile capacity while substantially reducing the associated uncertainty, owing to the smaller margin of error in load test measurements compared to that in predictions (Huang et al. 2016). Consequently, a low factor of safety (*FS*) in Allowable Stress Design, or a higher resistance factor in Reliability-based Design can be adopted if load tests are conducted. For instance, the *FS* can be reduced from 3.0–2.0 if the pile capacity calculated by empirical methods is confirmed by load tests (AASHTO 1998). Similarly, the resistance factor increases to 0.50–0.70 if static load tests are performed, in comparison to that of 0.35–0.45 if only static analysis is employed (CSA 2014).

The utilisation of pile load tests for the purpose of refining or validating designs bears a strong resemblance to the Bayesian statistical process. Prior knowledge of the pile capacity is formed using the design information, and pile load tests conducted during construction are utilised to update this prior knowledge. By combining existing knowledge of pile design with site-specific information from load tests, the reliability of piles can be updated (Zhang and Huang 2022; Zhang and Tang 2002). Bayesian methods have been employed to update the reliability of single piles based on pile load tests (Zhang, Li, and Tang 2006; Zhang, Huang, and Giacomini 2023). Zhang (2004) treated the mean pile capacity following a lognormal distribution and used the Bayesian method to update the pile capacity based on proof load tests. In contrast, Najjar and Gilbert (2009) assumed the pile capacity followed a mixed lognormal distribution and adopted the Bayesian method

CONTACT Jinsong Huang jinsong.huang@newcastle.edu.au

to update the lower-bound pile capacity. Results indicated that the proof load test significantly increased the reliability of piles, even if the test load was smaller than the predicted capacity. However, updating the reliability of pile groups based on pile load test results is rarely available in previous studies. A preliminary investigation on this topic was carried out in our previous work (Huang et al. 2016), which proposed a framework for updating the reliability of pile groups based on the individual pile load test results. However, the spatial variability of soils was not considered, leading to the correlation between individual pile capacities cannot be quantified as the correlation is influenced by soil properties.

In order to account for the spatial variability of soils in the reliability analysis of pile groups, a rigorous 3D finite difference (FD) method or finite element (FE) method may be required to assess the complex pile-soil-pile interaction, known as the group effect. However, the computational effort required is significant due to the complex numerical analysis that needs to be repeated numerous times to evaluate the updated reliability of pile groups, particularly for high reliability levels (e.g. reliability index, $\beta > 3$) (Huang et al. 2017). To address this issue, the group efficiency, $\eta$, is employed to reflect the group effect, defined as the ratio of the actual pile group capacity to the summation of the individual pile capacities (Poulos and Davis 1980). The concept of group efficiency has been utilised for a quick evaluation of the reliability of pile groups based on the behaviour of single piles (Bian et al. 2017; Huang et al. 2016; Oudah, El Naggar, and Norlander 2019). However, these studies predominantly relied on the assumption of a constant group efficiency value, disregarding its inherent complexity, which is influenced by various factors, such as the number of piles, group arrangement, and soil properties (Poulos, 1989; Sayed and Bakeer 1992). Additionally, previous studies concerning the estimation of group efficiency commonly treated the soil properties as deterministic (Kanellopoulos and Gazetas 2020; Rose, Taylor, and El Naggar 2013). Consequently, the group efficiency in the presence of spatially varying soil properties has not been assessed.

The correlation between pile capacities is another essential factor that affects the reliability of pile groups (Chen and Gilbert 2017; Klammler et al. 2013), but there is little guidance in the literature for quantifying the correlation coefficient. Thus, most previous studies adopted assumed values (e.g. 0, 0.5 or 1) and assigned the same correlation coefficient to piles within the pile group (Huang et al. 2016; Zhang, Tang, and Ng 2001). However, the pile capacity is primarily determined by the nearby soil property, such as undrained shear strength, $c_u$, which is known to be spatially correlated (Vanmarcke 2010). Therefore, it is more appropriate to consider that pile capacities are spatially correlated. Naghibi and Fenton (2017) used an isotropic Markov correlation function to describe the correlation between pile capacities within the group, and revealed the relationship between the reliability of single piles and the reliability of pile groups. Instead of directly treating the correlation coefficient as a spatially random variable, this paper considers the soil strength as a spatially random property, and the correlation between pile capacities is generated based on FD analysis results.

In this paper, a rigorous framework based on the random finite difference method (RFDM) and Bayes' theorem is proposed for updating the reliability of pile groups with load tests considering the spatial variability of soils. The FD analysis is merged with random field theory in conjunction with MCS to assess the statistics of group efficiency and pile capacity, as well as the correlation between pile capacities in spatially variable soils, which are further used in updating the reliability of pile groups with load test results based on Bayes' theorem. The first part of this paper introduces the methodology. The second part demonstrates the proposed approach for a 3×3 pile group subjected to axial loads in undrained clays. The reliability of pile groups updated by different load test results considering the spatial variability of soils is investigated.

## 2. Methodology

The proposed framework contains two parts: 1) updating the reliability of pile groups with load test results based on Bayes' theorem, and 2) assessing the statistics of group efficiency and pile capacity, as well as the correlation between pile capacities in spatially variable soils via RFDM. Further elaborations on these two parts are presented in the following subsections.

### 2.1. Updating reliability of pile groups with load test results

Suppose a pile group consists of $N$ piles, and the individual pile capacity ($y$) is assumed to be lognormally distributed with mean ($\mu_y$) and standard deviation ($\sigma_y$). The correlation coefficient between the capacities of pile $i$ and pile $j$ is denoted as $r_{ij}$, $i$ and $j = 1, 2, \ldots, N$. Thus, the joint probability density function of $N$ piles within the pile group is described as

follows (Huang et al. 2016):

$$f'_y(y_1, \ldots, y_N) = \frac{1}{(2\pi)^{N/2}\sqrt{|C|}\prod_{i=1}^{N} y_i} \times \exp\left\{-\frac{1}{2}(\ln y_i - \mu_{\ln y})^{\mathrm{T}} C^{-1}(\ln y_i - \mu_{\ln y})\right\} \quad (1)$$

where $|C|$ is the determinant of $C$, $\mu_{\ln y}$ is the mean of $\ln y$, superscript T means the transpose, $C$ is a $N$ by $N$ matrix with each element is defined as:

$$\begin{aligned} C_{ij} &= r_{ij}\sigma^2_{\ln y} \quad \text{if} \quad i \neq j \\ &= \sigma^2_{\ln y} \quad \text{if} \quad i = j \end{aligned} \quad (2)$$

where $\sigma_{\ln y}$ is the standard deviation of $\ln y$, $\sigma_{\ln y} = \sqrt{\ln(1 + COV_y^2)}$, $\mu_{\ln y} = \ln \mu_y - \frac{1}{2}\sigma^2_{\ln y}$ and $COV_y = \sigma_y/\mu_y$.

Two distinct types of pile groups are identified, namely: 1) free-standing group, wherein the pile cap is not in contact with the underlying soil; and 2) piled foundation, wherein the pile cap is in contact with the underlying soil. Only the free-standing group is considered herein, in which the cap-soil interaction does not need to be considered. The capacity of the free-standing pile group, $Q_{ug}$, is calculated based on the individual pile capacities and group efficiency (Poulos and Davis 1980):

$$Q_{ug} = \eta \sum_{i=1}^{N} y_i \quad (3)$$

Suppose a conventional Factor of Safety ($FS$) is adopted in the pile design. The load transfer from the superstructure is the mean capacity divided by $FS$. Thus, the limit state function ($g$) is defined as:

$$g = \eta \sum_{i=1}^{N} y_i - \frac{N\mu_y}{FS} \quad (4)$$

To be able to use Equations (1) and (4) to assess the reliability of pile groups, the values of $\eta$, $y$ and $r_{ij}$ in spatially variable soils should be evaluated. Thus, the RFDM is adopted, and the determination of these parameters is illustrated in section 2.3. The probability of failure, $p_f$, of the pile group cannot be obtained analytically. Thus, the Markov chain Monte Carlo (MCMC) method is adopted in this paper to sample the joint distribution. Once the individual pile capacities are sampled, Equation (4) is employed to evaluate the safety of the pile group. $g \leq 0$ implies that the pile group fails and $p_f$ is determined as the ratio of the number of failed simulations to the total number of simulations. It should be noted this paper focuses on the free-standing pile group with rigid cap subjected to axial loads. However, in cases where the cap is in contact with the underlying soils (i.e. piled foundation), or the cap is not strictly rigid, or the load condition is more generalised (e.g. combined lateral and axial loads), the limit state function needs to be replaced by appropriate numerical models, which are beyond the scope of this paper.

During construction, some load tests are conducted on single piles to verify the pile capacities, and the load test results are used to update the reliability of pile groups. The load test measurements are subject to errors and uncertainties. In this paper, the measurement error ($\varepsilon$) is assumed to be normally distributed with mean ($\mu_\varepsilon$) and standard deviation ($\sigma_\varepsilon$). The proof test load is assumed to be $T$. Thus, the actual load applied on the tested pile is $T - \varepsilon$. The likelihood function for a tested pile passes the proof load test is:

$$L \propto P(y \geq T - \varepsilon) = 1 - P(\varepsilon \leq T - y) = \Phi\left(\frac{\mu_\varepsilon - (T - y)}{\sigma_\varepsilon}\right) \quad (5)$$

where $\Phi$ is the cumulative distribution function of the standard normal distribution.

Suppose the proof load tests are conducted on $n$ piles with $m$ piles fail. The index of the failed pile is denoted as $f = (f_1, f_2, \cdots, f_m)$ while the index of the passed pile is denoted as $p = (p_1, p_2, \cdots, p_{n-m})$. The obtained test results (i.e. pass or fail) are denoted as the vector $\hat{y}$. Thus, the likelihood function for $m$ tests fail among $n$ tests is:

$$L(y_1, \ldots, y_N|\hat{y}) \propto \prod_{i=f_1}^{f_m}\left(1 - \Phi\left(\frac{\mu_\varepsilon - (T - y_i)}{\sigma_\varepsilon}\right)\right)\prod_{i=p_1}^{p_{n-m}}\Phi\left(\frac{\mu_\varepsilon - (T - y_i)}{\sigma_\varepsilon}\right) \quad (6)$$

Based on Bayes' theorem, the posterior distribution of $(y_1, \ldots, y_N)$ is derived as (Ang and Tang 2007):

$$\begin{aligned} f''_y(y_1, \ldots, y_N|\hat{y}) &\propto L(y_1, \ldots, y_N|\hat{y}) f'_y(y_1, \ldots, y_N) \\ &\propto \prod_{i=f_1}^{f_m}\left(1 - \Phi\left(\frac{\mu_\varepsilon - (T - y_i)}{\sigma_\varepsilon}\right)\right)\prod_{i=p_1}^{p_{n-m}}\Phi\left(\frac{\mu_\varepsilon - (T - y_i)}{\sigma_\varepsilon}\right) \\ &\quad \frac{1}{\prod_{i=1}^{N} y_i} \times \exp\left\{-\frac{1}{2}(\ln y_i - \mu_{\ln y})^{\mathrm{T}} C^{-1}(\ln y_i - \mu_{\ln y})\right\} \end{aligned} \quad (7)$$

The analytical derivation of the posterior distribution of pile capacity is not possible. Thus, the MCMC is utilised to directly sample the posterior distribution. Various MCMC algorithms exist, and the delayed rejection adaptive Metropolis (DRAM) algorithm proposed by Haario et al. (2006) is adopted, which is based on the

combination of the delayed rejection algorithm and the adaptive Metropolis algorithm. For detailed information on this method, interested readers can refer to the original paper by Haario et al. (2006).

## 2.2. Random finite difference method

### 2.2.1. Finite difference model

The capacity of a pile group is significantly different from the total capacity of individual piles due to the overlapping of stress and strain fields of neighbouring piles (Sayed and Bakeer 1992). Moreover, the failure mechanics of pile groups (e.g. block failure or individual pile failure) are complex, and empirical equations are not feasible for calculating the capacity of pile groups. Thus, FLAC3D (Itasca Consulting Group, 2017) is adopted in this paper to determine the capacity of pile groups. To be consistent, the capacity of single piles is also determined by FLAC3D.

A typical FD model of the single pile and pile group used in this paper is shown in Figure 1 (a) and (b), respectively. In order to simplify the process of generating a random field and mapping the randomly distributed soil property for each element, the soil medium is divided into 8-noded cubic elements with uniform size. While the incorporation of the complexity in random field generation resulting from an FD model with varying shapes and sizes of elements is possible, it is not addressed in this study. The soil is modelled using the Mohr-Coulomb plasticity model, while the pile is modelled using the pile-element, an inbuild structural element in FLAC3D. The pile-element represents the pile as a linear structural element with interface properties, and the physical geometry of piles does not need to be modelled. Pile-element modelling has been proven to significantly reduce computation time without losing accuracy for the analysis of pile groups (Maheetharan and Jaen-Toribio 2020). In light of the free-standing group considered herein, the pile cap does not need to be modelled in Figure 1 (b). To obtain the capacity of individual piles, the single pile FD model shown in Figure 1 (a) is utilised. In this analysis, a small incremental displacement is applied to the top of pile during each step. Simultaneously, the axial load on the pile is obtained using the embedded Fish function "force". The load-displacement curve of the pile is generated with a large number of steps (e.g. 50000) have been applied. Finally, the capacity is captured based on the load-displacement curve and specified failure criteria, e.g. ISSMFE criterion (ISSMFE 1985). A rigid pile cap is assumed to connect individual piles in this study, so that all piles undergo equal head displacements (Poulos, 1989). To obtain the capacity of the pile group, the pile group FD model shown in Figure 1 (b) is used. In this analysis, the same displacement is applied to the top of individual piles in each step. Simultaneously, the axial load on individual piles is obtained using the embedded Fish function "force" with the individual pile coordinates. The load-displacement curve of individual piles within the group is obtained when a large number of steps have been applied. The total load acted on the pile group is the summation of loads on individual piles (Zhang and Zhang 2012), while the displacement of the pile group is equivalent to that of individual piles. Consequently, a load-displacement curve for the pile group is obtained, and the same failure criterion utilised for individual piles is employed to define the capacity of the pile group.

When subjected to axial loads, piles transfer the external load to the soil medium through skin friction and end bearing. The skin friction is incorporated into the pile-element through the coupled shear spring

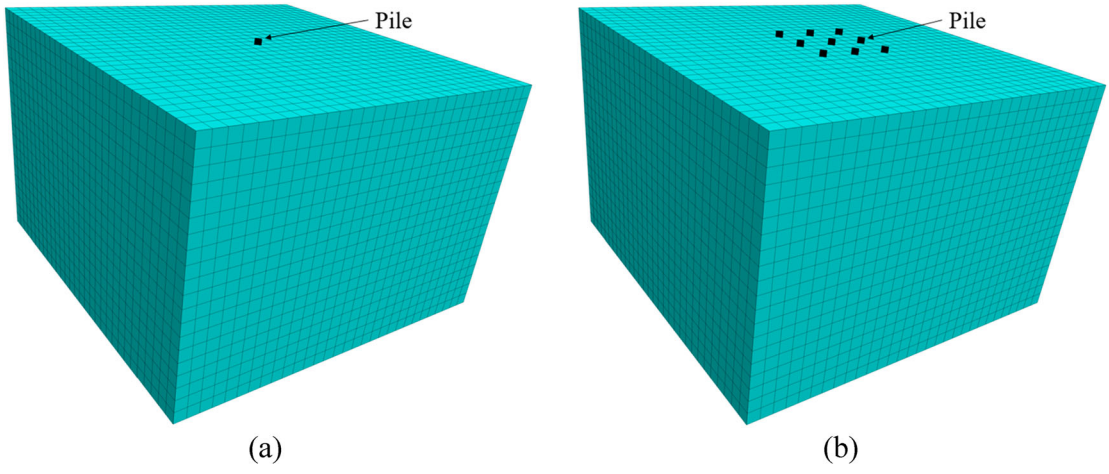


**Figure 1.** The FD model of the single pile and pile group.

along the pile length. The normal stiffness ($k_n$) and shear stiffness ($k_s$) are recommended by the FLAC3D manual (Itasca Consulting Group, 2017) as:

$$k_n \text{ or } k_s = 10 \times \max\left[\frac{K + 4G/3}{\Delta z_{\min}}\right] \tag{8}$$

where $K$ and $G$ are the bulk modulus and shear modulus of soil, respectively. $\Delta z_{\min}$ is the smallest dimension of an adjoining zone in the normal or shear direction.

The end bearing is incorporated into the pile-element through the coupled end bearing spring at the bottom of the pile. The minimum stiffness value of the end bearing spring ($k_b$) is set to be equal to or greater than the axial stiffness of the pile, as recommended by the FLAC3D manual (Itasca Consulting Group, 2017):

$$k_b = E_P A_b / L \tag{9}$$

where $E_P$ is the elastic modulus of the pile, $A_b$ is the area at the pile base, $L$ is the length of the pile.

#### 2.2.2. Random field model

Random fields have been frequently utilised to model the spatial variability of soil properties (Ching et al. 2021; Crisp et al. 2018; Vanmarcke 2010). Among various random field models, statistically homogeneous or stationary random fields are often preferred due to their relative simplicity and the practical feasibility of characterising them with limited data (Ching and Phoon 2013). Therefore, the stationary random field is adopted in this paper. For the pile foundations in undrained clay, the capacity of a pile or pile group is primarily dependent on the undrained shear strength, $c_u$. Therefore, in this paper, only $c_u$ is modelled as a random field while other parameters (e.g. elastic modulus) are treated as constant.

A three-dimensional (3D) stationary random field of $c_u$ can be characterised by the mean ($\mu_{c_u}$), coefficient of variation ($COV_{c_u}$) and spatial correlation length in three directions ($\theta_x$, $\theta_y$, $\theta_z$). In engineering practice, the mean and coefficient of variation of a random property are typically well understood. However, the spatial correlation length, also referred to as the scale of fluctuation, is often less comprehended (Lloret-Cabot, Fenton, and Hicks 2014). The spatial correlation length describes the distance over which the spatially random values in the underlying Gaussian field tend to be correlated. Conversely, two points that are separated by a distance exceeding the spatial correlation length are expected to be largely uncorrelated. Several covariance or correlation functions are available in the literature, such as the Markov correlation function, Triangular correlation function, and Gaussian correlation function (Fenton and Griffiths 2008). The Markov correlation function is widely used due to its simplicity, and thus is adopted in this paper. Notably, the use of isotropic spatial correlation lengths remains prevalent in the most recent publications on the reliability analysis of piles (Crisp, Jaksa, and Kuo 2021; Naghibi and Fenton 2022; Zhang et al. 2021). Furthermore, it is challenging to effectively demonstrate the influence of load test locations when a large vertical correlation length is employed. Additionally, the degree of anisotropy is inherently dependent on site-specific characteristics (Fenton and Griffiths 2005). Consequently, the isotropic spatial correlation length, $\theta_x = \theta_y = \theta_z = \theta$, is adopted in this study, while the consideration of the anisotropy correlation structure is left for future research. However, it should be noted that the proposed approach can be employed to consider anisotropic spatial correlation lengths. The isotropic Markov correlation function used in this paper is given as follows:

$$\rho(\tau) = \exp\left(-\frac{2|\tau|}{\theta}\right) \tag{10}$$

where $\rho(\tau)$ is the correlation coefficient between properties assigned to two points in the random field separated by an absolute distance $\tau$.

The lognormal distribution is usually used to characterise the variability of a soil property because it avoids a negative value for the soil property, which is not physically meaningful. Thus, the undrained shear strength $c_u$ is treated as lognormally distributed in this paper, which means the $\ln c_u$ is normally distributed. The mean ($\mu_{\ln c_u}$) and standard deviation ($\sigma_{\ln c_u}$) of the underlying normal distribution of $\ln c_u$ are obtained by: $\sigma_{\ln c_u} = \sqrt{\ln(1 + COV_{c_u}^2)}$ and $\mu_{\ln c_u} = \ln \mu_{c_u} - \frac{1}{2}\sigma_{\ln c_u}^2$.

In this paper, the generation of random fields is performed utilising the open-source toolbox "GSTools" (Müller et al. 2021). Initially, a standard normally distributed random field $G(x)$ is simulated through the randomisation method proposed by Kramer, Kurbanmuradov, and Sabelfeld (2007) and Heße et al. (2014). Subsequently, the desired lognormally distributed random field is obtained by transforming the underlying normally distributed random field using the following relationship:

$$c_{u_i} = \exp\left(\mu_{\ln c_u} + \sigma_{\ln c_u} G(x_i)\right) \tag{11}$$

where $x_i$ is a vector containing the coordinates of the $i$th element, $c_{u_i}$ is the desired undrained shear strength assigned to the $i$th element.

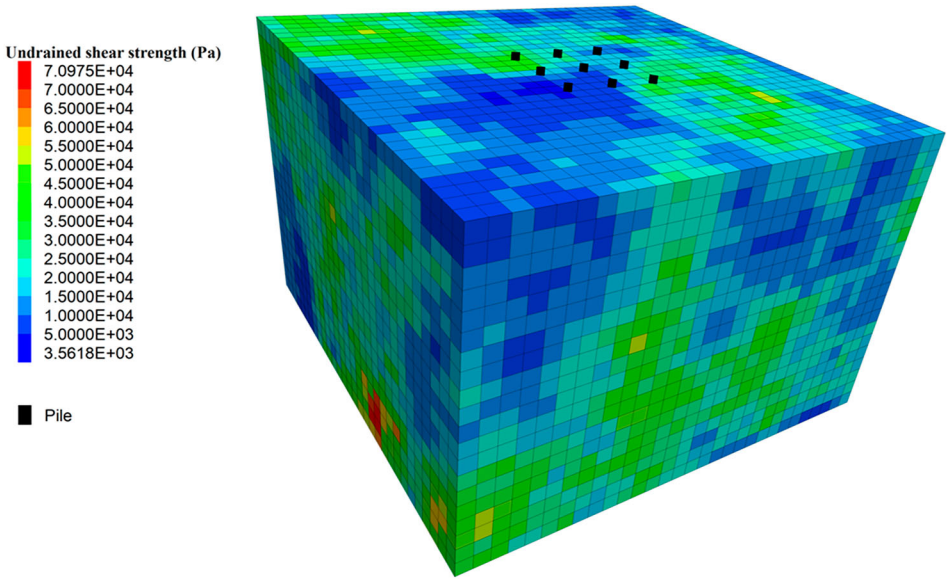


**Figure 2.** The pile group in spatially variable soils.

### 2.3. Evaluation of group efficiency, pile capacity and correlation between pile capacities

To evaluate the statistics of group efficiency and pile capacity, as well as the correlation between pile capacities in spatially variable soils, RFDM described in section 2.2 is utilised. The generation of random fields and the automation of MCS are based on Python programming, while the generation of the FE model and the mapping of random property for soil elements is based on the embedded FISH scripting language. The steps are summarised as follows:

Step 1: Generate the pile group model in FLAC3D and extract the coordinates of soil elements.

Step 2: Generate stationary random fields of $c_u$ based on the specified statistics of $c_u$.

Step 3: Extract the value of $c_u$ according to the coordinates of soil element and map the value to the corresponding soil element. A typical FD model of the pile group in spatially variable soils is shown in Figure 2.

Step 4: Use FLAC3D to compute the capacity of the pile group, following the process outlined in section 2.2.1. The pile group model presented in Figure 1 (b) is used to compute the capacity of the pile group, only one FD analysis is required.

Step 5: Use FLAC3D to compute the capacities of nine individual piles within the pile group in the same soil property, in accordance with the process described in section 2.2.1. The single pile model depicted in Figure 1 (a) is used to compute the capacity of individual piles, nine FD analyses are required owing to the variation of soils surrounding individual piles.

Step 6: Calculate the group efficiency based on the obtained capacity of pile group and individual piles.

Step 7: Repeat steps 2–6 for 100 times. The evaluation of the number of simulations is given in section 4.2.

Step 8: Derive the statistics of group efficiency (i.e. mean and coefficient of variation) based on the 100 group efficiency values.

Step 9: Generate the statistics of pile capacity (i.e. mean and coefficient of variation) based on the obtained 100 capacity values for nine individual piles. It should be noted that, despite the variation in capacities of individual piles across simulations, the underlying statistics of pile capacity for each pile remains constant because they are situated in the same random field.

Step 10: Generate the correlation coefficient between pile capacities based on the 100 combinations of the capacities of nine individual piles. Upon the completion of 100 simulations, a total of 100 combinations of the capacities of nine individual piles are generated, $(y_1^k, \ldots, y_9^k)$, $k = 1, 2, \ldots, 100$. The correlation coefficient $r_{ij}$, $i$ and $j = 1, 2, \ldots, 9$, is determined using the following equation (Ang and Tang 2007):

$$r_{ij} = \frac{\sum_{k=1}^{100} (y_i^k - \overline{y_i})(y_j^k - \overline{y_j})}{\sqrt{\sum_{k=1}^{100} (y_i^k - \overline{y_i})^2 \sum_{k=1}^{100} (y_j^k - \overline{y_j})^2}} \quad (12)$$

where $\overline{y_i} = \frac{1}{100}\sum_{k=1}^{100} y_i^k$ and $\overline{y_j} = \frac{1}{100}\sum_{k=1}^{100} y_j^k$.

## 3. Example

A 3×3 pile group subjected to axial loads in undrained clay is taken as an example to demonstrate the proposed approach. The pile length ($L$) is 10.5 m, with 10 m embedded in the clay, while the pile diameter ($D$) is 1.0 m. The pile spacing ($d$), is 3 times the pile diameter.

The elastic modulus ($E_P$) is determined as $2.2\times10^7$ kPa, while the Poisson ratio is 0.3. The soil medium is modelled as a cuboid of dimensions 30m×30m×20 m, which is discretized using cubic elements with a uniform side length of 1 m. The values of shear and bulk modulus are determined as $1.3\times10^3$ kPa and $6.0\times10^3$ kPa, respectively, following Bowles (1995).

In this paper, the spatial correlation length, $\theta$, is non-dimensionalized by dividing it by the embedded length of pile ($L_m = 10$m). The normalised spatial correlation length is denoted as $\Theta = \theta/L_m$. The value of $c_u$ assigned to each soil element in the FD model is treated as a random variable, with a mean value $\mu_{c_u} = 20$kPa, while $COV_{c_u}$ = 20%, 30%, 50% and 100%, and $\Theta$ = 0.5, 1, 2 and 5. It should be noted that the general range of $COV_{c_u}$ reported by Phoon and Kulhawy (1999) was 10%–55%, which is lower than that used in this paper. However, Fenton and Griffiths (2003) pointed out that $COV_{c_u}$ is related to the site investigation intensity and scale, and that even a value of $COV_{c_u}$ up to 5 is possible. Interested readers may refer to Fenton and Griffiths (2003) for further discussions on this topic.

When the statistics of group efficiency and pile capacity, as well as the correlation between pile capacities are obtained following section 2.3, these values are further used to update the reliability of pile groups by load test results following section 2.1. In this paper, the proof test load is assumed equal to the mean pile capacity, $T = \mu_y$, and the $FS$ used in the design is assumed equal to 2, $FS = 2$. The mean and standard deviation of measurement error are assumed as 0 and $0.1T$, $\mu_\varepsilon = 0$ and $\sigma_\varepsilon = 0.1T$, respectively. It should be noted that the measurement error is related to the load test method (e.g. dynamic or static load tests), as well as the method to interpolate the $t$-$z$ (load-displacement) curve obtained by load tests. However, there is little guidance on quantifying the value of measurement error, and further research is needed to address this issue.

## 4. Results

### 4.1. Group efficiency in deterministic soils

In this section, the evaluation of group efficiency, $\eta$, in deterministic soils is presented. The results are then compared with those obtained by empirical formulas to validate the FD model employed in this paper.

This study investigates $\eta$ at three displacement levels, specifically $0.05D$, $0.075D$ and $0.10D$. The selected displacement level is used to define the capacity of individual piles and the pile group. For example, when assessing the group efficiency at the displacement level of $0.05D$, the capacity of individual piles and the pile group is defined as the load corresponding to a displacement of $0.05D$. The selection of these specific displacement levels is based on previous studies that have highlighted variations in $\eta$ concerning different displacement levels (Comodromos 2004; Rose, Taylor, and El Naggar 2013). It is noteworthy that a displacement level beyond $0.10D$ is not considered because the majority of load has been mobilised by a displacement of $0.10D$ (Fleming et al. 2009). A uniform value of $c_u = 20$kPa is used in this section. $\eta$ for different spacing-to-diameter ratios ($d/D$) and displacement levels are assessed and presented in Figure 3. It is observed that $\eta$ varies with the displacement level of pile groups, as observed by Rose, Taylor, and El Naggar (2013). Results also reveal that $\eta$ in clay soils are below unity, which is consistent with the observations made by Poulos and Davis (1980). Additionally, it is shown that $\eta$ increases as $d/D$ increases. For the group efficiency determined based on the displacement equals $0.05D$, the group efficiency increases from 0.42–0.90 as $d/D$ increases from 1.5–5. For $d/D = 8$, the group efficiency approaches 1, which means group effect is minimal at a larger pile spacing.

Several empirical formulas have been proposed to estimate $\eta$, which is summarised in Table 1. Among these, the formulas proposed by Bolin (1941) and Feld (1943) relied solely on the spacing-to-diameter ratio and number of piles, with the same parameters used but in different formulations. On the other hand, the formula developed by Seiler and Keeney (1944) only considered the pile spacing and number of piles, while ignoring the pile diameter. It is found that this formula is invalid for the case of $a = b = 1$, as it yields a $\eta$ of 1.15, contrary to the fact that $\eta$ should be unity for a single pile. Poulos and Davis (1980) incorporated the

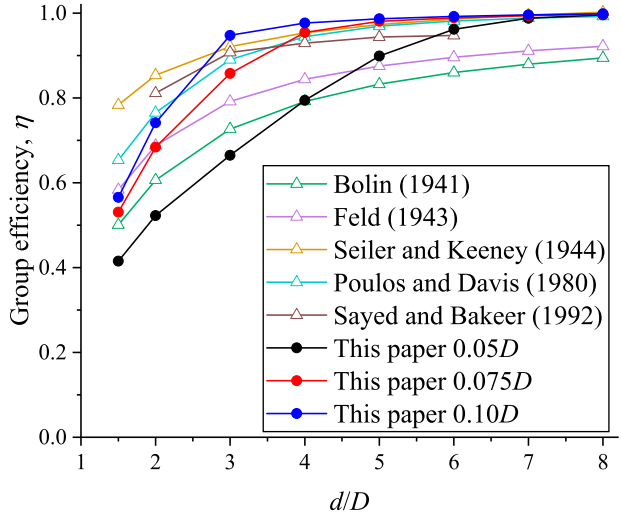


**Figure 3.** Comparison of $\eta$ by deterministic analysis and empirical formulas.

**Table 1.** Summary of empirical formulas for group efficiency.

| Reference | Formulas |
|---|---|
| Bolin (1941) | $\eta = 1 - \left[\frac{(b-1)a + (a-1)b}{90ab}\right]\tan^{-1}\left(\frac{D}{d}\right)$ |
| Feld (1943) | $\eta = 1 - \frac{D}{\pi dab}[a(b-1) + b(a-1) + \sqrt{2}(a-1)(b-1)]$ |
| Seiler and Keeney (1944) | $\eta = \left\{1 - \left[\frac{11d}{7(d^2-1)}\right]\left[\frac{a+b-2}{a+b-1}\right]\right\} + \frac{0.3}{a+b}$ |
| Poulos and Davis (1980) | $\frac{1}{\eta^2} = 1 + \frac{(ab)^2 P_1^2}{P_B^2}$ |
| Sayed and Bakeer (1992) | $\eta = 1 - (1 - \eta'_s \cdot K)\varsigma$<br>$\eta'_s = 2\frac{[(b-1)d + D] + [(a-1)d + D]}{\pi abD}$ |

Note: $a$ is the number of rows of the pile group, $b$ is the number of piles per row, $P_1$ is the capacity of a single pile, $P_B$ is the capacity for block failure of the group, $\eta'_s$ is the geometric efficiency, $K$ is the group interaction factor, $\varsigma$ is the friction factor.

failure mechanism of the pile group in their calculation of $\eta$. The $P_B$ is the capacity for block failure of the group, which assumes the soil enclosing the pile group perimeter acts as a rigid block upon failure. In a different approach, Sayed and Bakeer (1992) proposed two new parameters (i.e. $K$ and $\varsigma$) to consider the effect of the property and type of soil, pile length, and method of pile installation. However, these parameters may lead to subjective results.

For comparison purposes, $\eta$ calculated using these empirical formulas is also presented in Figure 3. Results reveal that $\eta$ calculated using different formulas are considerably inconsistent. For example, when $d/D = 2$, $\eta$ is 0.61, given by Bolin (1941), whereas 0.85 is obtained by Seiler and Keeney (1944). For $d/D \geq 3$, $\eta$ obtained by FLAC3D with a displacement level equal to $0.10D$ is slightly higher than those obtained using empirical formulas. This can be attributed to the small pile length to diameter ratio used in the model, as indicated by Poulos and Davis (1980). Generally, the results presented in this paper are in line with those obtained using empirical formulas.

### 4.2. Group efficiency in spatially variable soils

In this section, the evaluation of $\eta$ in spatially variable soils is carried out. The value of $c_u$ assigned to each soil element in the FD model is treated as a spatially random variable, with a constant mean value $\mu_{c_u} = 20$kPa, while $COV_{c_u} =$ 20%, 30%, 50% and 100%, and $\Theta =$ 0.5, 1, 2 and 5. The pile capacity is defined by the ISSMFE criterion (ISSMFE 1985), corresponding to the displacement of pile group is $0.10D$.

The number of simulations carried out for each set of statistical values (i.e. $\mu_{c_u}$, $COV_{c_u}$ and $\Theta$) significantly

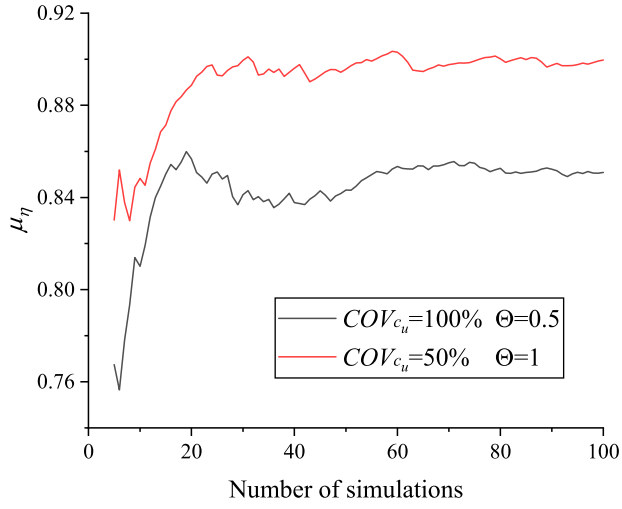


**Figure 4.** Effect of the number of simulations on $\mu_\eta$.

affects the accuracy of the estimated statistics of $\eta$. An estimate based on a few numbers of simulations will lead to a large standard deviation, whereas a large number of simulations requires extensive computation time. Figures 4 and 5 show the effect of the number of MCS on the mean ($\mu_\eta$) and coefficient of variation ($COV_\eta$) of $\eta$, respectively. It is observed that the fluctuation of $\mu_\eta$ and $COV_\eta$ is negligible when 70 simulations are used. Thus, 100 simulations are deemed adequate for this study.

Figure 6 shows how $\mu_\eta$ varies with $COV_{c_u}$ and $\Theta$ for $d/D = 3$. It can be seen that $\mu_\eta$ in spatially variable soil is generally lower than that obtained from the deterministic analysis. It also shows that $\mu_\eta$ decreases as $COV_{c_u}$ increases. For example, $\mu_\eta$ is 0.94 when $COV_{c_u} = 20\%$ and $\Theta = 1$, while $\mu_\eta$ is 0.82 when $COV_{c_u} = 100\%$ and $\Theta = 1$. Additionally, it can be observed that $\mu_\eta$ first decreases and then increases as $\Theta$ increases from 0.5–

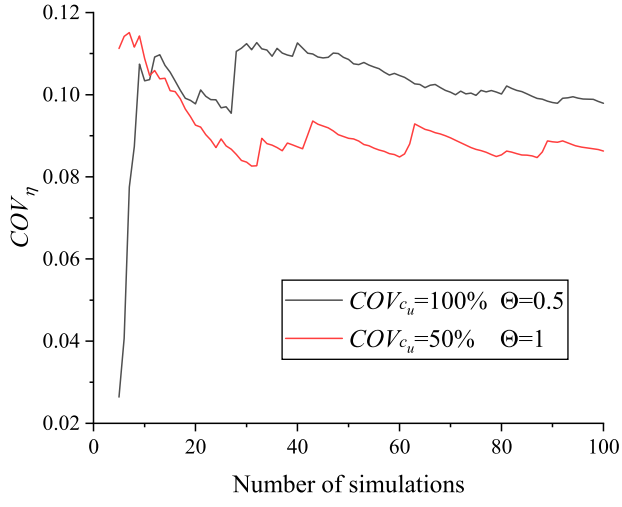


**Figure 5.** Effect of the number of simulations on $COV_\eta$.

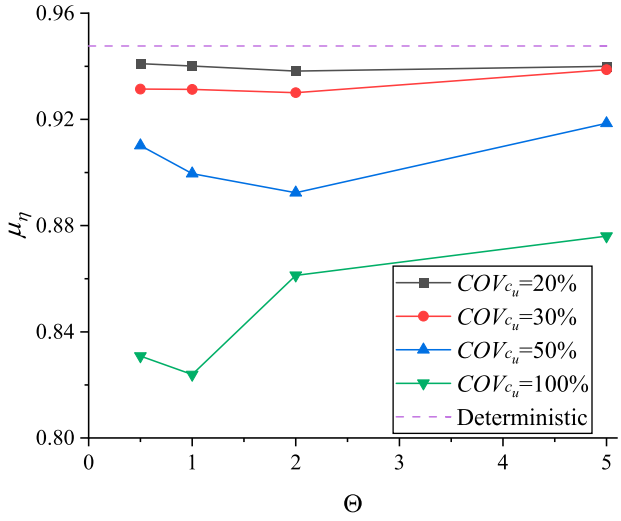


**Figure 6.** $\mu_\eta$ as a function of $COV_{c_u}$ and Θ.

5. Specifically, for $COV_{c_u} = 50\%$, $\mu_\eta$ decreases from 0.91–0.89 as Θ increases from 0.5–2, and then increases to 0.92 as Θ increases to 5. The value of Θ corresponding to the greatest reduction in $\mu_\eta$ falls within the range of 1–2.

The variation of $COV_\eta$ with respect to $COV_{c_u}$ and Θ for $d/D = 3$ is presented in Figure 7. It is noted that $COV_\eta$ exhibits an increasing trend as Θ increases. Specifically, for $COV_{c_u} = 100\%$, $COV_\eta$ increases from 0.10–0.16 as Θ increases from 0.5–5. Furthermore, it is found that the effect of $COV_{c_u}$ on $COV_\eta$ is significant, and $COV_\eta$ increases as the $COV_{c_u}$ increases. For instance, for $\Theta = 2$, $COV_\eta$ is 0.03, 0.05, 0.09 and 0.16 when $COV_{c_u}$ is equal to 20%, 30%, 50% and 100%, respectively. This observation can be attributed to the relationship between $\eta$ and the soil strength (Poulos, 1989). As the variability

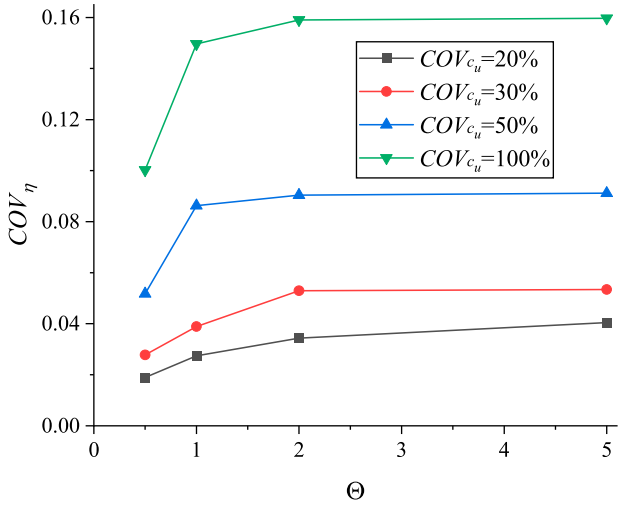


**Figure 7.** $COV_\eta$ as a function of $COV_{c_u}$ and Θ.

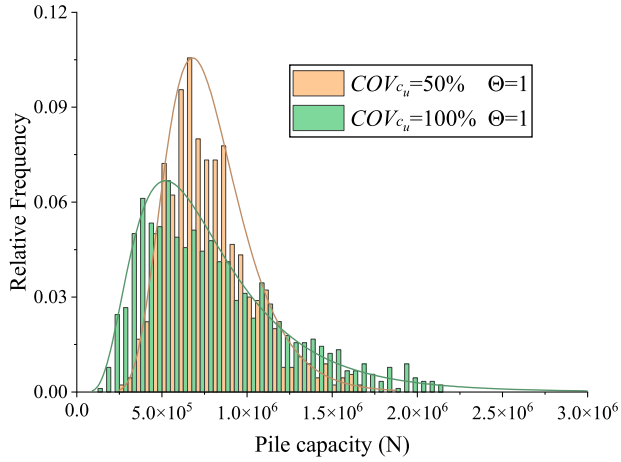


**Figure 8.** The distribution of the single pile capacity.

of soil increases, it is expected that $\eta$ will exhibit a corresponding increase in variability.

### 4.3. The statistics of pile capacity and the correlation between pile capacities

Figure 8 shows the histogram of the single pile capacity with $COV_{c_u} = 50\%$ and 100%, and $\Theta = 1$. The lognormal distribution is utilised to fit the pile capacity, and it demonstrates that the lognormal distribution fits the histogram quite well. Additionally, it shows that the mean pile capacity is only slightly different for $COV_{c_u} = 50\%$ and $COV_{c_u} = 100\%$ (i.e. 799kN and 787kN), as observed by Fenton and Griffiths (2007). In contrast, the pile capacity spreads over a larger area for $COV_{c_u} = 100\%$, implying that the variation of pile capacity, $COV_y$, increases as $COV_{c_u}$ increases, which is reasonable as the soil becomes increasingly variable, its ability to support the pile would also become increasingly variable.

The assessment of the correlation coefficient between pile capacities, $r_{ij}$, is conducted in accordance with Step 10 outlined in section 2.3. Figure 9 illustrates the correlation coefficient for $COV_{c_u} = 50\%$, $\Theta = 1$ and 2. It is noted that Θ has a significant effect on the correlation coefficient. An increase in Θ indicates that the strength of soil is correlated over a wider area, resulting in the pile capacities that are determined based on the strength property being more likely to be correlated. Specifically, the correlation coefficient between pile 1 and pile 3 is 0.41 for $\Theta = 1$, but it increases to 0.70 as Θ increases to 2. It is noted that the correlation coefficient between pile capacities is related to the distance between piles. For example, the distance between pile 1 and pile 2 (or pile 4) is the smallest, and the correlation coefficient is the highest. Conversely, the distance between pile 1 and pile 9 is the largest, and the correlation coefficient is the lowest.

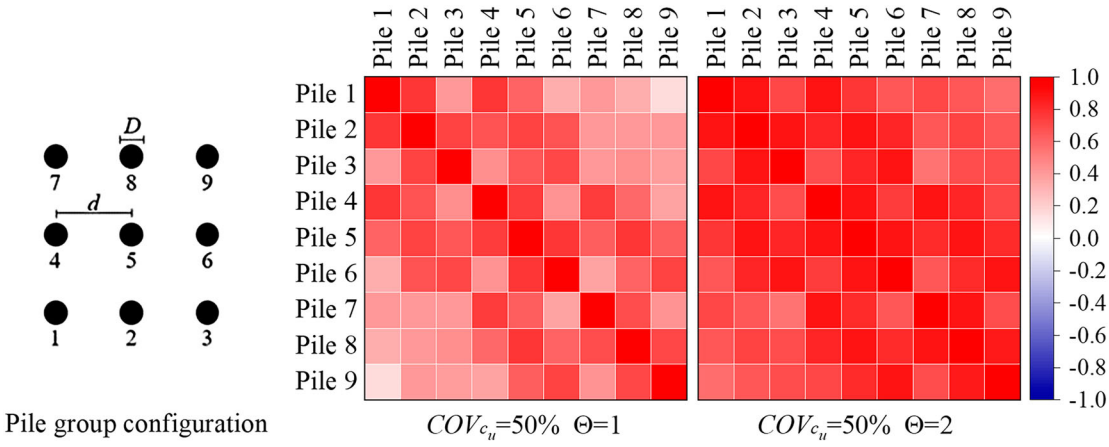


**Figure 9.** The correlation coefficient between pile capacities.

**Table 2.** Updated individual pile capacities based on load tests.

| Cases | | Prior | Posterior | | | | | |
|---|---|---|---|---|---|---|---|---|
| | | | Pile 1 | Pile 2/4 | Pile 3/7 | Pile 5 | Pile 6/8 | Pile 9 |
| Case 1: $\Theta = 5$ $m = 0$ | Mean | 1.00 | 1.36 | 1.34 | 1.31 | 1.32 | 1.29 | 1.26 |
| | COV | 0.41 | 0.27 | 0.29 | 0.31 | 0.30 | 0.32 | 0.34 |
| Case 2: $\Theta = 5$ $m = 1$ | Mean | 1.00 | 0.73 | 0.75 | 0.77 | 0.76 | 0.78 | 0.80 |
| | COV | 0.41 | 0.24 | 0.26 | 0.30 | 0.28 | 0.31 | 0.33 |
| Case 3: $\Theta = 0.5$ $m = 0$ | Mean | 1.00 | 1.19 | 1.10 | 1.03 | 1.06 | 1.01 | 1.00 |
| | COV | 0.24 | 0.17 | 0.22 | 0.24 | 0.23 | 0.24 | 0.24 |
| Case 3: $\Theta = 0.5$ $m = 1$ | Mean | 1.00 | 0.84 | 0.92 | 0.98 | 0.95 | 0.99 | 1.00 |
| | COV | 0.24 | 0.16 | 0.22 | 0.24 | 0.23 | 0.24 | 0.24 |

### *4.4. Reliability of pile groups updated by load test results*

Based on the obtained group efficiency (section 4.2), the pile capacity and the correlation coefficient between pile capacities (section 4.3), the reliability of pile group updated by different load test results is investigated in the section. It should be noted that, in Table 2 and Figures 10–13, the load tests are assumed to be conducted following the order of piles within the pile group, wherein the first test is conducted on pile 1, and the second test is conducted on pile 2. In contrast, in Figures 14 and 15, the load tests are conducted on the designated pile without adherence to the order of piles.

With the completion of load tests, the individual pile capacities are updated based on the test outcomes. Table 2 summarises the updated individual pile capacities for different spatial correlation lengths and test results, with $n = 1$ and $COV_{c_u} = 50\%$. The load test is assumed to be conducted on pile 1. Consequently, owing to the symmetrical configuration of the pile group, the updated results for pile 2 and pile 4, pile 3 and pile 7, as well as pile 6 and pile 8, are identical. The mean values shown in Table 2 are normalised by their respective prior mean values, thus consistently yielding prior mean values of 1 across all cases. Table 2 reveals that the posterior mean and coefficient of variation (COV) of individual pile capacities are significantly influenced by their relative distances from the tested pile. For example, in Case 1, where pile 2 and pile 4, being the closest to pile 1, exhibit higher mean capacities and lower COV in contrast to pile 9, situated at a greater distance. Additionally, it is noteworthy that the spatial correlation length also exerts an impact on the posterior

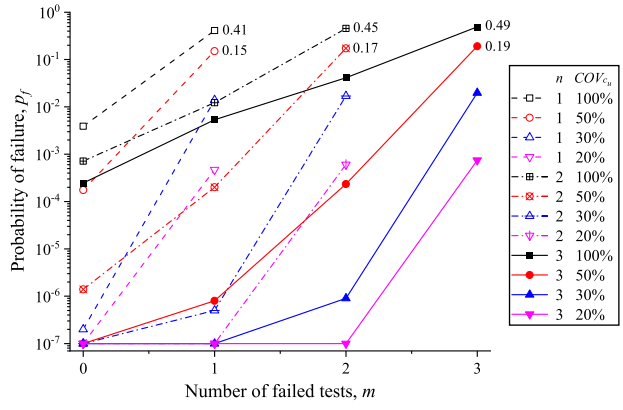


**Figure 10.** $p_f$ updated by different load test results with various $COV_{c_u}$.

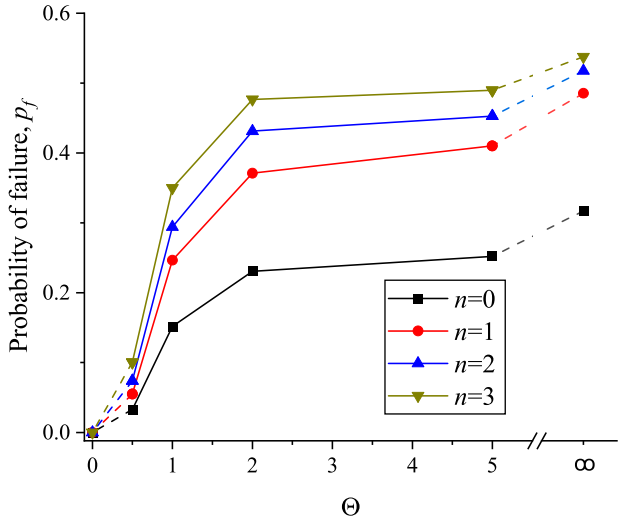


**Figure 11.** $p_f$ as a function of the number of load tests (all fail), and Θ.

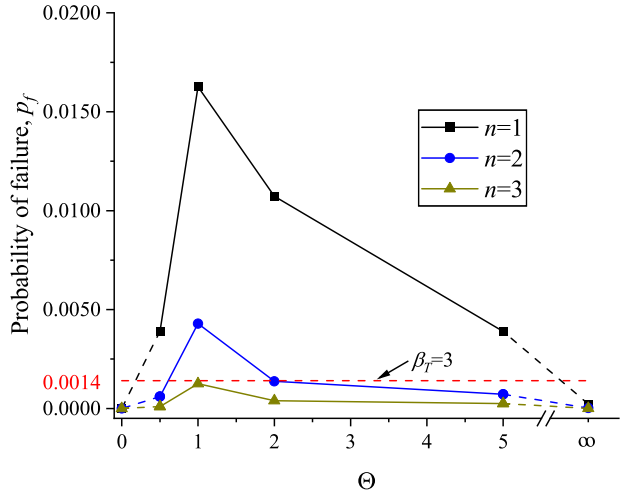


**Figure 13.** $p_f$ as a function of the number of load tests (all pass), and Θ.

mean and COV of individual pile capacities. For instance, the test result significantly affects pile 9 in Case 1 and Case 2, where $\Theta = 5$, while the test result has no effect on pile 9 in Case 3 and Case 4, where $\Theta = 0.5$. Furthermore, results in Table 2 elucidate that a tested pile passes the load test increases the mean pile capacity, while a tested pile fails the load test decreases the mean pile capacity. Remarkably, a reduction in the variation of pile capacity is consistently observed with load tests conducted, regardless of test outcomes.

Figure 10 shows how $p_f$ varies with $COV_{c_u}$, the number of load tests, $n$, and the number of failed tests, $m$, for $\Theta = 5$. In light of the utilisation of ten million simulations in the probability analysis, values of $p_f$ less than 1.0e-7 cannot be determined through simple MCS. Consequently, these values are represented as $p_f = 1.0\text{e-}7$ in Figure 10, where the y-axis employs a logarithmic scale. Figure 10 shows that, for the same $n$ and $m$, $p_f$ increases as $COV_{c_u}$ increases. For example, when three load tests are conducted and all piles fail, $p_f$ are 7.46e-4, 0.02, 0.19, and 0.49 for $COV_{c_u} = 20\%$, $COV_{c_u} = 30\%$, $COV_{c_u} = 50\%$ and $COV_{c_u} = 100\%$, respectively. It is noteworthy that, when $COV_{c_u} = 20\%$, the pile group still satisfies the design requirement (e.g. a target reliability index, $\beta_T = 3$, or $p_f \leq 0.0014$) even if three consecutive piles fail, indicating that the $FS = 2$ used in the soil with small $COV_{c_u}$ is conservative. Moreover, Figure 10 indicates that the test results have a significant effect on $p_f$. For instance, when $n = 3$ and $COV_{c_u} = 100\%$, $p_f$ increases from 2.46e-4–0.49 as $m$ increases from zero to three.

Figure 11 illustrates the change of $p_f$ with respect to $n$ and Θ for $COV_{c_u} = 100\%$. It is assumed that all the

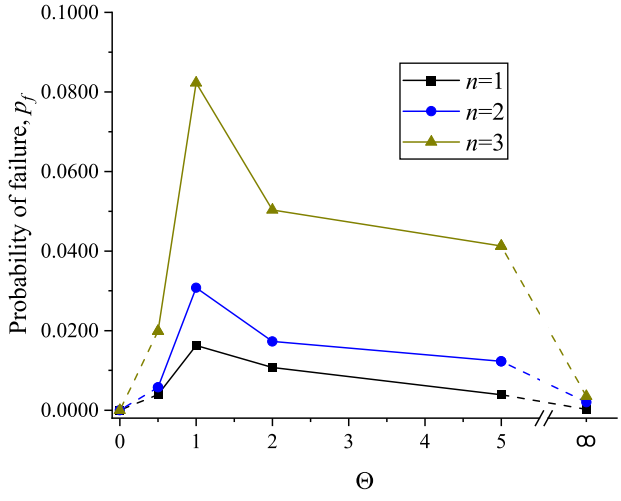


**Figure 12.** $p_f$ as a function of the number of load tests (only the last test passes), and Θ.

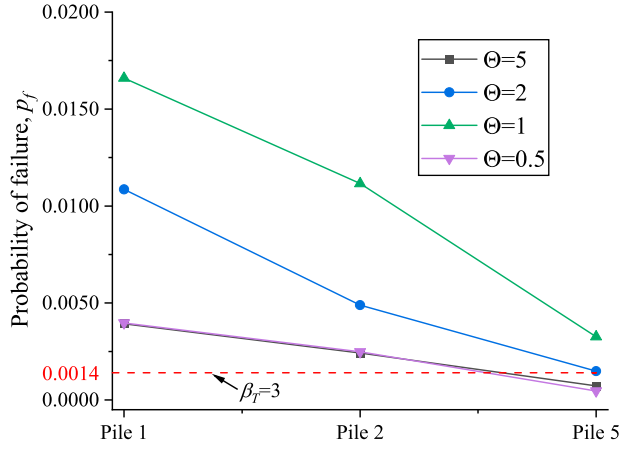


**Figure 14.** The effect of load test location on $p_f$, for $n = 1$ and $m = 0$.

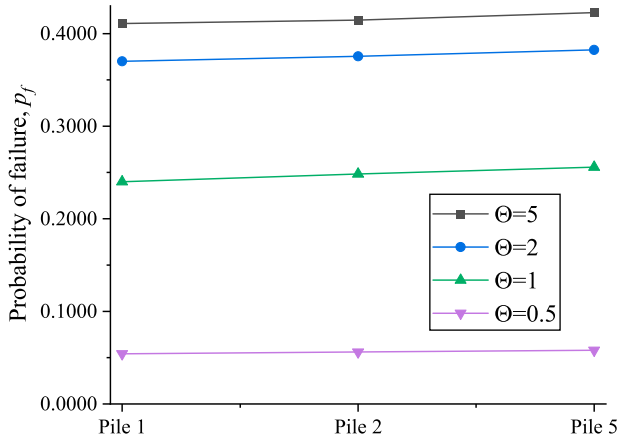


**Figure 15.** The effect of load test location on $p_f$, for $n = 1$ and $m = 1$.

tested piles fail (i.e. $n = m$). When no tests conducted ($n = 0$), $p_f < 1.0\text{e-}7$ as $\Theta \to 0$, which can be analysed as follows: when $\Theta$ approaches zero, the variation in $c_u$ is eliminated owing to the averaging effect (Fenton and Griffiths 2005). Consequently, the coefficient of variation of the pile capacity, $COV_y$, and group efficiency, $COV_\eta$, tend towards zero. Moreover, the pile group capacity based on the mean of $c_u$ is consistently exceeds the design value when $FS = 2$ is employed, resulting in $p_f = 0$. When three consecutive piles fail, $p_f$ remains zero for $\Theta \to 0$ in Figure 11. This is mainly because the individual piles are uncorrelated, the test results do not impact untested piles. Even if three consecutive piles fail, the presence of strong piles compensates for the weak ones, ensuring the safety of the pile group. For the opposite extreme case, $\Theta \to \infty$, each simulation of MCS involves a uniform soil, with the value of $c_u$ is randomly sampled from its distribution. In this case, $COV_y$ and $COV_\eta$ are non-zero because the pile capacity and group efficiency are influenced by the soil strength, resulting in a non-zero value of $p_f$ as depicted in Figure 11. Additionally, Figure 11 reveals a monotonic increase in $p_f$ with increasing $\Theta$ while the worst-case phenomenon is not pronounced. The results indicate that ignoring spatial variation (i.e. $\Theta \to \infty$) leads to an overestimation of $p_f$. From a reliability-based design perspective, the worst-case spatial correlation length occurs when $\Theta \to \infty$.

Figures 12 and 13 depict the variation in $p_f$ with respect to $n$ and $\Theta$ for $COV_{c_u} = 100\%$. In Figure 12, it is assumed that only the last tested pile passes the proof load test, while in Figure 13, all the tested piles pass the proof load test (i.e. $m = 0$). In contrast to the monotonic relationship observed in Figure 11, both Figure 12 and Figure 13 exhibit a non-monotonic trend. $p_f$ initially increases and subsequently decreases as $\Theta$ increases. The worst-case phenomenon is pronounced in Figure 12 and Figure 13 with the worst-case spatial correlation length corresponding to $\Theta = 1$. The results presented in Figure 12 and Figure 13 indicate that ignoring spatial variation (i.e. $\Theta \to \infty$) underestimates $p_f$, which may lead to an unconservative design.

Based on the results depicted in Figure 13, it can be deduced that $\Theta$ plays a critical role in determining the optimal number of tests required to attain a target reliability for the pile group (e.g. $\beta_T = 3$ or $p_f \leq 0.0014$). Notably, for $\Theta = 0.5$ and 5, the pile group can meet the design requirement with two consecutive piles passing the tests. In contrast, for $\Theta = 1$ and 2, achieving the desired reliability index requires that at least three consecutive piles pass the tests.

This part aims to illustrate the effect of load test locations on $p_f$, which refers to situations wherein the tested pile does not follow the order of piles. Figures 14 and 15 show the effect of load test locations (i.e. pile 1/corner pile, pile 2/edge pile and pile 5/centre pile) on $p_f$ for $COV_{c_u} = 100\%$ and $n = 1$. It is assumed that the tested pile passes (i.e. $m = 0$) in Figure 14 while the tested pile fails (i.e. $m = 1$) in Figure 15. Notably, regardless of the value of $\Theta$, the load test conducted on pile 5 consistently yields the minimum value of $p_f$ if the pile passes (i.e. Figure 14), while it consistently yields the maximum value of $p_f$ if the pile fails (i.e. Figure 15). The observation indicates that the load test on pile 5 provides more information regarding the reliability of pile groups, suggesting that the centre pile is the optimal location if only one test is to be performed. In contrast, previous studies have failed to consider the spatial variability of soils, leading to an assumption of perfect correlation among individual pile capacities. Consequently, the potential impact of load test locations on the updated reliability of pile groups has been disregarded.

It is worth noting that the load test location affects the required number of load tests to achieve the target reliability of pile groups. For instance, in Figure 14, when $\Theta = 5$, $p_f = 3.92\text{e-}3$ if pile 1 is tested while $p_f = 7.22\text{e-}4$ if pile 5 is tested. In this case, if the target reliability index of 3 (i.e. $p_f \leq 0.0014$) is adopted in pile design, the result obtained based on the load test on pile 5 is sufficient to verify the design of pile groups. However, if the load test is conducted on pile 1 or pile 2, more load tests are required.

It is noted that the results for $\Theta$ of 0.5 and 5 exhibit almost identical outcomes in Figure 14, which can be explained as follows. In the extreme case, where $\Theta \to 0$, the values of $c_u$ at any two distinct points are independent. In this case, the pile effectively averages the $c_u$ field, resulting in individual pile capacities tending to those obtained in a deterministic condition

(Fenton and Griffiths 2005). Consequently, the tested pile is quite representative of the untested piles, and a pass of the tested pile indicates a low $p_f$ for the pile group. Conversely, in the extreme case, where $\Theta \to \infty$, individual pile capacities exhibit perfect correlation. In this case, a pass of the tested pile implies a higher likelihood that the untested piles will also pass the tests, thereby yielding a low $p_f$ again. However, at intermediate correlation lengths, the tested pile becomes a less accurate estimator of the untested piles, leading to an increase in $p_f$. Consequently, $p_f$ initially increases and subsequently decreases as $\Theta$ increases from zero to infinity, with the highest $p_f$ occurring at an intermediate correlation length between zero and infinity. Figure 14 illustrates that the highest $p_f$ corresponds to $\Theta = 1$. Hence, the results for $\Theta = 0.5$ and 5 may appear similar.

## 5. Conclusions

This paper proposes a rigorous framework for updating the reliability of pile groups with load tests, accounting for the spatial variability of soil. The group efficiency, pile capacity and correlation between pile capacities in spatially variable soils are evaluated, which are further utilised in updating the reliability of pile groups based on the number of tests and the corresponding test results. Results indicate that neglecting the spatial variability (assuming $\Theta \to \infty$) leads to an overconservative design when all piles fail. Conversely, it results in an unconservative design when one or more piles pass. These findings underscore the importance of incorporating spatial variability into the evaluation of pile group reliability.

The proposed approach allows for the consideration of the impact of load test locations on the updated reliability of pile groups, surpassing the limitations of previous studies. Notably, for a 3×3 pile group, results indicate that the centre pile is the optimal location if only one test is to be performed. However, it should be noted that the present investigation regarding the effect of load test locations involves only one load test, and a comprehensive investigation into the optimal load test scheme (e.g. the number of tests and corresponding test locations) remains a topic for future research.

## Disclosure statement

No potential conflict of interest was reported by the author(s).

## Funding

This work was supported by the National Natural Science Foundation of China (Project Nos. 41972280, 42272326). The first author wishes to acknowledge support from the China Scholarship Council (grant number 201906270257).

## References

AASHTO. 1998. *LRFD Bridge Design Specifications Foundation*. 2nd ed. Washington, D.C.: American Association of State Highway and Transportation Officials.

Ang, A. H.-S., and W. H. X. Tang. 2007. *Probability Concepts in Engineering Planning and Design: Emphasis on Application to Civil and Environmental Engineering*. Hoboken, NJ: Wiley.

Bian, X.-y., J.-j. Zheng, R.-J. Zhang, and Z.-j. Xu. 2017. "Reliability Analysis for Serviceability Limit State of Pile Groups Foundation." *KSCE Journal of Civil Engineering* 22 (1): 54–61. https://doi.org/10.1007/s12205-017-0246-1.

Bolin, H. W. 1941. "The Pile Efficiency Formula of the Uniform Building Code." *Building Standards Monthly* 10 (1): 4–5.

Bowles, J. E. 1995. *Foundation Analysis and Design*.

Chen, J. B., and R. B. Gilbert. 2017. "Offshore Pile System Model Biases and Reliability." *Georisk-Assessment and Management of Risk for Engineered Systems and Geohazards* 11 (1): 55–69. https://doi.org/10.1080/17499518.2016.1250914.

Ching, J., and K.-K. Phoon. 2013. "Probability Distribution for Mobilised Shear Strengths of Spatially Variable Soils Under Uniform Stress States." *Georisk: Assessment and Management of Risk for Engineered Systems and Geohazards* 7 (3): 209–224. https://doi.org/10.1080/17499518.2013.801273.

Ching, J., K.-K. Phoon, Z. Yang, and A. W. Stuedlein. 2021. "Quasi-site-specific Multivariate Probability Distribution Model for Sparse, Incomplete, and Three-Dimensional Spatially Varying Soil Data." *Georisk: Assessment and Management of Risk for Engineered Systems and Geohazards* 16 (1): 53–76. https://doi.org/10.1080/17499518.2021.1971256.

Comodromos, E. M. 2004. "Response Evaluation of Axially Loaded Fixed Head Pile Groups Using 3D Nonlinear Analysis." *Soils and Foundations* 44 (2): 31–39. https://doi.org/10.3208/sandf.44.2_31.

Crisp, M. P., M. B. Jaksa, and Y. L. Kuo. 2021. "Characterising Site Investigation Performance in Multiple-Layer Soils and Soil Lenses." *Georisk-Assessment and Management of Risk for Engineered Systems and Geohazards* 15 (3): 196–208. https://doi.org/10.1080/17499518.2020.1806332.

Crisp, M. P., M. B. Jaksa, Y. L. Kuo, G. A. Fenton, and D. V. Griffiths. 2018. "A Method for Generating Virtual Soil Profiles with Complex, Multi-Layer Stratigraphy." *Georisk: Assessment and Management of Risk for Engineered Systems and Geohazards* 13 (2): 154–163. https://doi.org/10.1080/17499518.2018.1554817.

CSA. 2014. "Canadian Highway Bridge Design Code." In *CSA-S6-14*, edited by Canadian Standards Association, 231–232. Mississauga, ON: Code and Commentary.

Feld, J. 1943. "Discussion on Friction Pile Foundations." *Transactions of the American Society of Civil Engineers* 108 (1): 73–115. https://doi.org/10.1061/TACEAT.0005589

Fenton, G. A., and D. V. Griffiths. 2003. "Bearing-capacity Prediction of Spatially Random c – ϕ Soils." *Canadian Geotechnical Journal* 40 (1): 54–65. https://doi.org/10.1139/t02-086.

Fenton, G. A., and D. V. Griffiths. 2005. "Three-dimensional Probabilistic Foundation Settlement." *Journal of Geotechnical and Geoenvironmental Engineering* 131 (2): 232–239. https://doi.org/10.1061/(Asce)1090-0241(2005)131:2(232).

Fenton, G. A., and D. V. Griffiths. 2007. "Reliability-based Deep Foundation Design." In *Probabilistic Applications in Geotechnical Engineering*, 1–12. https://doi.org/10.1061/40914(233)1.

Fenton, G. A., and D. V. Griffiths. 2008. *Risk Assessment in Geotechnical Engineering*. New York: John Wiley & Sons.

Fleming, W. G. K., A. J. Weltman, M. F. Randolph, and W. K. Elson. 2009. *Piling Engineering*. 3rd ed. Abingdon: Taylor and Francis.

Haario, H., M. Laine, A. Mira, and E. Saksman. 2006. "DRAM: Efficient Adaptive MCMC." *Statistics and Computing* 16 (4): 339–354. https://doi.org/10.1007/s11222-006-9438-0.

Heße, F., V. Prykhodko, S. Schlüter, and S. Attinger. 2014. "Generating Random Fields with a Truncated Power-law Variogram: A Comparison of Several Numerical Methods." *Environmental Modelling & Software* 55: 32–48. https://doi.org/10.1016/j.envsoft.2014.01.013.

Huang, J. S., G. Fenton, D. V. Griffiths, D. Q. Li, and C. B. Zhou. 2017. "On the Efficient Estimation of Small Failure Probability in Slopes." *Landslides* 14 (2): 491–498. https://doi.org/10.1007/s10346-016-0726-2.

Huang, J. S., R. Kelly, D. Q. Li, C. B. Zhou, and S. Sloan. 2016. "Updating Reliability of Single Piles and Pile Groups by Load Tests." *Computers and Geotechnics* 73: 221–230. https://doi.org/10.1016/j.compgeo.2015.12.003.

ISSMFE. 1985. "Axial Pile Loading Test—Part 1: Static Loading." *Geotechnical Testing Journal* 8 (2): 79–90. https://doi.org/10.1520/GTJ10514J.

Itasca Consulting Group, I. 2017. *FLAC3D — Fast Lagrangian Analysis of Continua in Three-Dimensions, Ver. 6.0. Minneapolis: Itasca*.

Kanellopoulos, K., and G. Gazetas. 2020. "Vertical Static and Dynamic Pile-to-Pile Interaction in non-Linear Soil." *Geotechnique* 70 (5): 432–447. https://doi.org/10.1680/jgeot.18.P.303.

Klammler, H., M. McVay, R. Herrera, and P. Lai. 2013. "Reliability Based Design of Driven Pile Groups Using Combination of Pile Driving Equations and High Strain Dynamic Pile Monitoring." *Structural Safety* 45: 10–17. https://doi.org/10.1016/j.strusafe.2013.07.009.

Kramer, P. R., O. Kurbanmuradov, and K. Sabelfeld. 2007. "Comparative Analysis of Multiscale Gaussian Random Field Simulation Algorithms." *Journal of Computational Physics* 226 (1): 897–924. https://doi.org/10.1016/j.jcp.2007.05.002.

Länsivaara, T., K. K. Phoon, and J. Ching. 2021. "What is a Characteristic Value for Soils?" *Georisk: Assessment and Management of Risk for Engineered Systems and Geohazards* 16 (2): 199–224. https://doi.org/10.1080/17499518.2021.1975301.

Lloret-Cabot, M., G. A. Fenton, and M. A. Hicks. 2014. "On the Estimation of Scale of Fluctuation in Geostatistics." *Georisk: Assessment and Management of Risk for Engineered Systems and Geohazards* 8 (2): 129–140. https://doi.org/10.1080/17499518.2013.871189

Maheetharan, A. T. A., and A. Jaen-Toribio. 2020. "Verification of Pile Modelling Technique in FLAC3D." In *Applied Numerical Modeling in Geomechanics*, edited by D. Billaux, J. Hazzard, M. Nelson, and M. Schöpfer. Paper, 16–03.

Müller, S., L. Schüler, A. Zech, and F. Heße. 2021. "GSTools v1. 3: A Toolbox for Geostatistical Modelling in Python." *Geoscientific Model Development Discussions*, 1–33. https://doi.org/10.5194/gmd-2021-301.

Naghibi, F., and G. A. Fenton. 2017. "Target Geotechnical Reliability for Redundant Foundation Systems." *Canadian Geotechnical Journal* 54 (7): 945–952. https://doi.org/10.1139/cgj-2016-0478.

Naghibi, F., and G. A. Fenton. 2022. "Design of Foundations Against Differential Settlement." *Canadian Geotechnical Journal* 59 (3): 384–396. https://doi.org/10.1139/cgj-2020-0782.

Najjar, S. S., and R. B. Gilbert. 2009. "Importance of Proof-Load Tests in Foundation Reliability." In *Contemporary Topics in In Situ Testing, Analysis, and Reliability of Foundations*, 340–347. https://doi.org/10.1061/41022(336)44.

Oudah, F., M. H. El Naggar, and G. Norlander. 2019. "Unified System Reliability Approach for Single and Group Pile Foundations - Theory and Resistance Factor Calibration." *Computers and Geotechnics* 108: 173–182. https://doi.org/10.1016/j.compgeo.2018.12.003.

Phoon, K. K., and F. H. Kulhawy. 1999. "Characterization of Geotechnical Variability." *Canadian Geotechnical Journal* 36 (4): 612–624. https://doi.org/10.1139/t99-038.

Phoon, K. K., and C. Tang. 2019. "Characterisation of Geotechnical Model Uncertainty." *Georisk-Assessment and Management of Risk for Engineered Systems and Geohazards* 13 (2): 101–130. https://doi.org/10.1080/17499518.2019.1585545.

Poulos, H. G. 1989. "Pile Behavior - Theory and Application." *Geotechnique* 39 (3): 363–415. https://doi.org/10.1680/geot.1989.39.3.365.

Poulos, H. G., and E. H. Davis. 1980. *Pile Foundation Analysis and Design*.

Rose, A. V., R. N. Taylor, and M. H. El Naggar. 2013. "Numerical Modelling of Perimeter Pile Groups in Clay." *Canadian Geotechnical Journal* 50 (3): 250–258. https://doi.org/10.1139/cgj-2012-0194.

Sayed, S. M., and R. M. Bakeer. 1992. "Efficiency Formula for Pile Groups." *Journal of Geotechnical Engineering-Asce* 118 (2): 278–299. https://doi.org/10.1061/(Asce)0733-9410(1992)118:2(278).

Seiler, J. F., and W. D. Keeney. 1944. "The Efficiency of Piles in Groups." *Wood Preserving News* 22 (11): 109–118.

Vanmarcke, E. 2010. *Random Fields: Analysis and Synthesis*. Beijing: World scientific.

Zhang, L. M. 2004. "Reliability Verification Using Proof Pile Load Tests." *Journal of Geotechnical and Geoenvironmental Engineering* 130 (11): 1203–1213. https://doi.org/10.1061/(Asce)1090-0241(2004)130:11(1203).

Zhang, Y., and J. Huang. 2022. Calibration of Resistance Factor Based on Pile Load Test Conducted to Failure. 8th International Symposium on Geotechnical Safety and Risk (ISGSR), Newcastle, Australia.

Zhang, Y., J. Huang, and A. Giacomini. 2023. "Bayesian Updating on Resistance Factors of H-Piles with Axial Load Tests." *Computers and Geotechnics* 159. https://doi.org/10.1016/j.compgeo.2023.105421.

Zhang, X.-l., B.-h. Jiao, Y. Han, S.-l. Chen, and X.-y. Li. 2021. "Random Field Model of Soil Parameters and the Application in Reliability Analysis of Laterally Loaded Pile." *Soil Dynamics and Earthquake Engineering* 147: 106821. https://doi.org/10.1016/j.soildyn.2021.106821.

Zhang, L. M., D. Q. Li, and W. H. Tang. 2006. "Level of Construction Control and Safety of Driven Piles." *Soils and Foundations* 46 (4): 415–425. https://doi.org/10.3208/sandf.46.415.

Zhang, L., and W. H. Tang. 2002. *Use of Load Tests for Reducing Pile Length* Deep Foundations 2002: An International Perspective on Theory, Design, Construction, and Performance.

Zhang, L. M., W. H. Tang, and C. W. W. Ng. 2001. "Reliability of Axially Loaded Driven Pile Groups." *Journal of Geotechnical and Geoenvironmental Engineering* 127 (12): 1051–1060. https://doi.org/10.1061/(Asce)1090-0241(2001)127:12(1051).

Zhang, Q.-q., and Z.-m. Zhang. 2012. "Simplified Calculation Approach for Settlement of Single Pile and Pile Groups." *Journal of Computing in Civil Engineering* 26 (6): 750–758. https://doi.org/10.1061/(asce)cp.1943-5487.0000167.